JOURNAL OF MATERIALS SCIENCE 31 (1996) 6005–6013

Carbothermal nitridation synthesis of α-Si_3N_4 powder from pyrolysed rice hulls

A. W. WEIMER*, J. R. CASSIDAY‡, D. W. SUSNITZKY§, C. K. BLACK, D. R. BEAMAN¶
Ceramics and Advanced Materials Research, The Dow Chemical Company, Midland, MI 48667, USA

The carbothermal nitridation synthesis of α-Si_3N_4 was studied using a high-temperature tube furnace to react a precursor, comprised of pyrolysed rice hulls (C/SiO_2) and additive "seed" Si_3N_4, with N_2. The experimental design for synthesis was a three-level factorial surface response design for determining the effect of temperature (1300–1380 °C) and reaction time (1–5 h) on kinetics. In addition, all precursors were reacted at 1460, 1480 and 1500 °C for 5 h in order to ensure high conversion suitable for product powder evaluation (composition and morphology). Following excess carbon removal, the product Si_3N_4 was >95% α-phase and had a surface area of 7.7 $m^2 g^{-1}$ with an oxygen content of 3.6 wt% O. The powder was comprised of a bimodal size distribution of submicrometre solid α-Si_3N_4 crystallites centred at 0.03 and 0.22 μm. No whiskers or high aspect ratio elongated crystallites were found in the powder. The addition of carbon black to the seeded pyrolysed rice hull C/SiO_2 mixture had no significant impact on the reaction rate or product powder properties. The reaction was modelled using a nuclei–growth rate expression as

$$(kt)^{0.58} = -\ln(1 - X)$$

$$k = 1.09 \times 10^{10} \exp(-50502/T)$$

where (1573 K < T < 1653 K), (3600 < t < 18000 s), (0 < X < 1), and k = rate in s^{-1}.

1. Introduction

There is substantial interest in the development of a low-cost production process for sinterable Si_3N_4 powder used in low-temperature applications [1]. Such a powder could contain higher levels of impurities such as oxygen, carbon, and metals. In terms of carbothermal nitridation synthesis, this process should utilize inexpensive C/SiO_2 raw materials and have a higher reactor throughput than that normally achieved for the synthesis of a high-purity Si_3N_4 product powder. The study reported here was carried out to evaluate the use of rice hulls which are a readily available, inexpensive, and renewable source of intimately mixed carbon and silica.

Rice hulls, a by-product of the paddy mill, are a unique agricultural waste [2, 3]. About 20 wt% of paddy is removed as husk by milling and about 18 wt% of the husk is ash which is primarily comprised of SiO_2. The silica enters the rice plant through its roots in a soluble form probably as a silicate or monosilicic acid and then moves to the outer surface of the plant where it becomes concentrated by evaporation and polymerization to form cellulose silica membrane. In the conversion of rice husk to ash, the oxidation process removes the organic matter and leaves a silica residue. Although the main components of rice hulls are organic materials, they produce, on pyrolysis (calcination under inert conditions, i.e. nitrogen), an intimate mixture of carbon and silica (C/SiO_2). The yield and composition (of the C/SiO_2) from rice hull pyrolysis depend on the variety, climate, and geographical location [4] of the grown rice. Typically, the C/SiO_2 ratio is such that an excess of carbon above the stoichiometric requirement for synthesizing Si_3N_4 is available for reaction.

The synthesis of Si_3N_4 and SiC from pyrolysed rice hulls has been reported in detail by various investigators [2, 5–14]. With the exception of Rahman and Riley [12], the previous work using pyrolysed rice hulls for the synthesis of Si_3N_4 has not included the use of additive "seed" Si_3N_4 in the precursor

*Author to whom all correspondence should be addressed. *Present address*: Department of Chemical Engineering, University of Colorado, Boulder, CO 80309, USA.
‡*Present address*: Dow Corning Corporation, Midland, MI, USA.
§*Present address*: Intel Corporation, Santa Clara, CA, USA.
¶*Present address*: Beaman Associates, Heber City, UT, USA.

0022–2461

formulation. Without "seed" present, undesirable whiskers comprise a substantial part of the product.

In this study, washed rice hulls were obtained from a commercial supplier. They were pyrolysed and used in the precursor formulation "as-is". No acid leaching steps were carried out to remove contaminants prior to reaction. The pyrolysed rice hulls were blended with "seed" Si_3N_4 and reacted at higher temperatures in flowing nitrogen using a laboratory tube furnace. The product Si_3N_4 was "burned out" in air to remove residual carbon, and analysed (chemical composition and morphology). It should be understood that there was nothing special about the particular rice hulls purchased and processed in this study. Lower and higher grades of rice hulls are most likely available from other vendors.

2. Experimental procedure

2.1. Precursor preparation

Washed rice hull flour (120 mesh) was obtained from Composition Materials of America, Inc. (Montgomery, AI). It was then pyrolysed in flowing nitrogen at 800 °C for 4 h. The resulting powder was used as the C/SiO_2 source for the precursor formulations. A 75.9% weight loss was experienced during the pyrolysis of the rice hulls. The properties of the pyrolysed rice hulls are summarized in Table I.

Assuming that the oxygen is in the form of SiO_2 and that the pyrolysed rice hull powder contains only carbon and SiO_2, its composition can be normalized to 30.2 wt% C and 69.8 wt% SiO_2. Pyrolysed rice hulls are believed to be one of the least expensive intimate mixtures of carbon and silica available for use as a precursor to Si_3N_4 and SiC.

Five precursor formulations were prepared using the pyrolysed rice hulls as the C/SiO_2 source and Si_3N_4 seed in a "seed"/SiO_2 = 0.2 weight ratio. The precursors also contained starch as a binder. The difference in the precursors was in the amount of additional carbon black added as excess. The "as-is" pyrolysed powder comprised an excess carbon content of 5.8% above the stoichiometric requirement. Additional precursors were made containing 10%, 25%, 50% and 75% excess carbon. Each precursor was ball-milled for 5 h in a urethane-lined jar using Si_3N_4 media. Following the ball-milling step, the powder was separated from the media and placed in a mortar where it was blended with deionized water using a pestle. Once the desired consistency of powder and water was reached, the wet precursor was formed into aggregates. The wet aggregates were dried overnight at 150 °C and then pyrolysed in a tube furnace at 330 °C for 3 h in flowing nitrogen. The formulation for each aggregate batch is shown in Table II.

TABLE II Precursor powder composition

Precursor (% excess C)	Added carbon black (g)[a]	Pyrolysed rice hulls (g)	"Seed" Si_3N_4 (g)[b]
5.8	0	74.77	10.43
10	0.34	74.46	10.40
25	2.62	72.46	10.12
50	26.33	226.98	31.69
75	1.98	64.26	8.97

[a]98.6 wt% C; 72 $m^2 g^{-1}$, high purity (< 100 p.p.m. total metals).
[b] > 90% α-Si_3N_4; 10.1 $m^2 g^{-1}$; 1.23 wt% O; high purity (< 100 p.p.m. total metals).

2.2. Horizontal tube furnace description

The Si_3N_4 synthesis was carried out in the laboratory scale tube furnace as shown in Fig. 1. The furnace used was a CM 1725 horizontal tube furnace containing a 7.62 cm outer diameter (o.d.) × 0.762 m long SiC tube. The tube had a 7.62 cm long hot zone which was heated by eight molybdenum disilicide heating elements. This SiC tube was used to prevent cracking associated with thermal shock during insertion of a cold graphite reactor crucible into the hot heated tube (to be discussed). Control of the furnace was provided by a Honeywell UDC 3000 and a CM 106 over temperature controller, both of which used type B thermocouples.

Nitrogen gas flowed continuously into the reactor crucible through a 1.27 cm o.d. graphite pipe inserted through a water-cooled steel flange comprising the side of the SiC furnace tube. Nitrogen gas flowed at the rate of 6 l min^{-1} through the graphite reaction crucible. This graphite pipe was threaded into the graphite reactor crucible which held approximately 14 g calcined precursor pellets. This 5.72 cm o.d. × 7.62 cm long crucible reactor could slide inside the SiC tube. The crucible had two end caps which could be unscrewed to allow the addition or removal of precursor aggregates. The base of the aggregate holding section contained drilled holes which allowed for nitrogen gas to flow through the aggregates during reaction. A downstream nominal 1.27 cm o.d. × 15.24 cm piece of graphite pipe reduced back diffusion of reactor tube gases into the reactor crucible. Exhaust gas flowed through a knock-out container and a bubbler which allowed visual verification of nitrogen flow.

2.3. Silicon nitride synthesis and excess carbon removal

The overall stoichiometric equation for the carbothermal nitridation synthesis of Si_3N_4 is as follows

$$3SiO_2 + 2N_2 + 6C \rightarrow Si_3N_4 + 6CO \quad (1)$$

TABLE I Pyrolysed rice hulls properties

Carbon (%)	Oxygen (%)	Nitrogen (%)	Aluminium (%)	Calcium (%)	Iron (p.p.m.)	Surface area ($m^2 g^{-1}$)
30.4	37.3	1.0	0.13	1.3	930	91.9

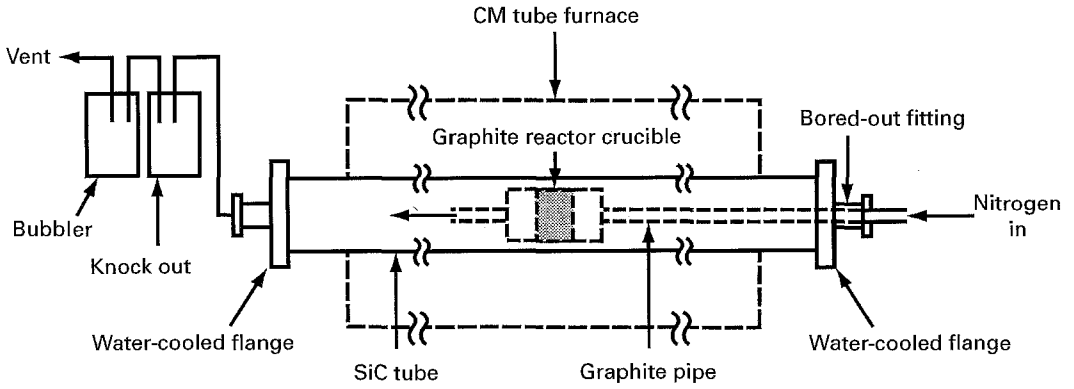

Figure 1 Laboratory horizontal tube furnace apparatus.

This reaction is envisaged to proceed via a nucleation and growth process. First, SiO is formed at the contact points of C and SiO_2

$$SiO_2(s) + C(s) \rightarrow SiO(g) + CO(g) \quad (2)$$

Once CO is formed, SiO may form by the reduction of SiO_2 with CO

$$SiO_2(s) + CO(g) \rightarrow SiO(g) + CO_2 \quad (3)$$

$$C(s) + CO_2(g) \rightarrow 2\,CO(g) \quad (4)$$

The SiO reacts to form new Si_3N_4 nuclei in the following manner:

$$3\,C(s) + 3\,SiO(g) + 2\,N_2(g) \rightarrow Si_3N_4(s) + 3\,CO_2(g) \quad (5)$$

If the reaction occurs at a pre-existing nucleus, then a gas-phase growth reaction will occur

$$3\,CO(g) + 3\,SiO(g) + 2\,N_2(g) \rightarrow Si_3N_4(s) + 3\,CO_2(g) \quad (6)$$

For each reaction, approximately 14 g precursor were loaded into a graphite crucible. The reactor was then assembled so that the graphite crucible was initially at least 30.5 cm away from the hot zone. The reactor was then brought up to the desired temperature at a heating rate of $20\,^{\circ}C\,min^{-1}$. When the desired temperature was reached, the crucible was inserted into the hot zone. The reaction crucible was maintained at the desired temperature for the selected length of time. At the end of the reaction, the furnace was cooled at a rate of $50\,^{\circ}C\,min^{-1}$ to room temperature.

An experimentally defined matrix of experiments was carried out for the two independent variables of time (1–5 h) and temperature (1380–1460 °C). The centrepoint of the experimental matrix (3 h at 1420 °C) was repeated three times. This matrix was applied only to the 50% and 5.8% excess carbon runs. In addition, each precursor was reacted for 5 h at 1480 and 1500 °C to ensure high SiO_2 conversion. In order to obtain low conversions, the precursors containing 5.8%, 10%, 25% and 50% excess carbon were reacted at 1340 °C for 1, 3 and 5 h. In addition, the 5.8% excess carbon precursor was reacted at 1300 °C for 1, 3, and 5 h.

For data analysis purposes, the product was assumed to be comprised of a mixture of Si_3N_4, unreacted SiO_2, and carbon. To remove the excess carbon, the reacted precursor was crushed with a pestle, loaded into a quartz boat and "burned out" with a flowing air/N_2 mixture (80/20) in a laboratory tube furnace at 550 °C for 3 h. All free carbon was oxidized to CO_2 in 3 h calcining.

2.4. Analytical characterization and data analysis

Carbon analysis of the synthesized Si_3N_4 was carried out using a LECO HF 400 and LECO IR 412 carbon determinator (LECO Corporation). Sample material is combusted with released CO converted to CO_2 in a rare-earth copper oxide catalytic heater. Carbon is then measured as CO_2 by infrared analysis. Reaction product analysis for oxygen was completed using a LECO EF 400 and a LECO 436 oxygen/nitrogen determinator. The sample was pyrolysed and released oxygen combined with carbon to form CO. The CO was converted to CO_2 as described above, and the oxygen was measured by infrared spectroscopy in the form of CO_2.

The Si_3N_4 powder morphology was examined by field-emission gun scanning electron microscopy (FEG/SEM) using a Topcon DS-130F operated at 2.0–3.0 kV and by transmission electron microscopy (TEM) using a Topcon EM-002B operated at 200 kV. A mean-number crystallite diameter, after Russ [15] was determined using randomly obtained transmission electron micrographs. The powder particles to be sized were selected by overlaying a grid on to each photomicrograph and then measuring the size of particles that were intersected by the grid.

Surface area was determined by the BET nitrogen adsorption method using an Autosorb-1 (Quantochrome Corp.) surface area analyser and following standard manufacturer's procedures. Trace metal impurities were quantified by X-ray fluorescence using a Kevex 0700 XRF spectrometer with analysis carried out using a Philip's PW1404 XRF spectrometer for metals. The XRF-11 Criss Software package was used for matrix corrections and to calculate the results. Particle-size distribution measurements were made using a Microtrac II model 158705 particle size analyser (Leeds and Northrup). Powder was first dispersed in deionized water and sonicated using a Sonabox

TABLE III Final product properties for 5.8% "as-is" precursor reacted for 5 h at 1460 °C

Carbon (wt%)	Oxygen (wt%)	Nitrogen (wt%)	Ca (p.p.m.)	Al (p.p.m.)	Fe (p.p.m.)	α-Si_3N_4 (%)	Surface area ($m^2 g^{-1}$)
0.51	3.61	38.76	7900	1900	2000	> 95	7.7

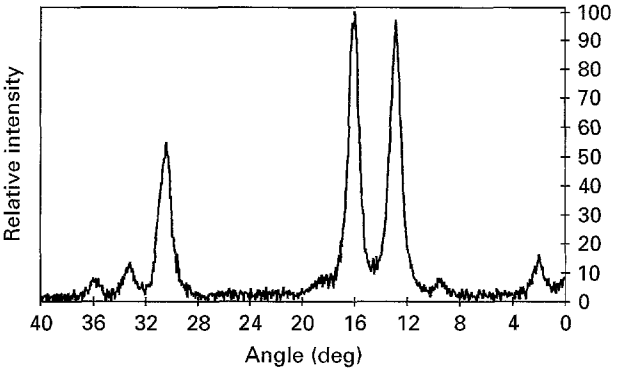

Figure 2 X-ray diffraction pattern for Si_3N_4 from "as-is" pyrolysed rice hulls (5 h at 1460 °C; precursor "seed"/SiO_2 = 0.2).

II (Artek Systems Corporation) sonicator. Crystal-phase purity was determined by X-ray diffraction (Ragaku "Miniflex" X-ray diffractometer).

To quantify the degree of conversion, the product powder after burn-out was assumed to be comprised only of Si_3N_4, unreacted SiO_2 and free carbon. The fractional carbon conversion, X, is calculated from the reaction weight loss, "burn-out" weight loss, carbon analysis of the precursor and after "burn-out", and oxygen analysis after "burn-out". The method is similar to that utilized by Tsukada *et al.* [16].

3. Results and discussion

3.1. Final product properties

Maximum conversion was achieved by all precursors when reacted at temperatures of 1460, 1480, and 1500 °C for 5 h. Product powder properties of the "as-is" 5.8% excess carbon precursor reacted at 1460 °C for 5 h are summarized in Table III.

An X-ray diffraction pattern for this powder is shown in Fig. 2. A desirable high α-Si_3N_4 phase purity of > 95% is indicated. The metallic impurities of 1900 p.p.m. Al and 2000 p.p.m. Fe are consistent with low-cost Si_3N_4 powders (e.g. Denka SN-9S at 2000 p.p.m. Fe and Al) on the market today. The higher oxygen content of 3.61 wt% O may be acceptable for lower temperature applications [1] as it is well known that impurities, especially oxygen, have little or no effect on performance up to at least several hundred degrees centigrade. The 0.51 wt% carbon might be in the form of nanophase SiC and as such may be beneficial. The powder had a surface area of 7.7 $m^2 g^{-1}$, as indicated in Table III.

Photomicroscopy (FEG/SEM and TEM) (Figs 3–6) indicated that the powder was comprised of submicrometre crystallites. No whiskers or elongated high aspect ratio crystallites were detected. The FEG/SEM image shown in Fig. 3 at different

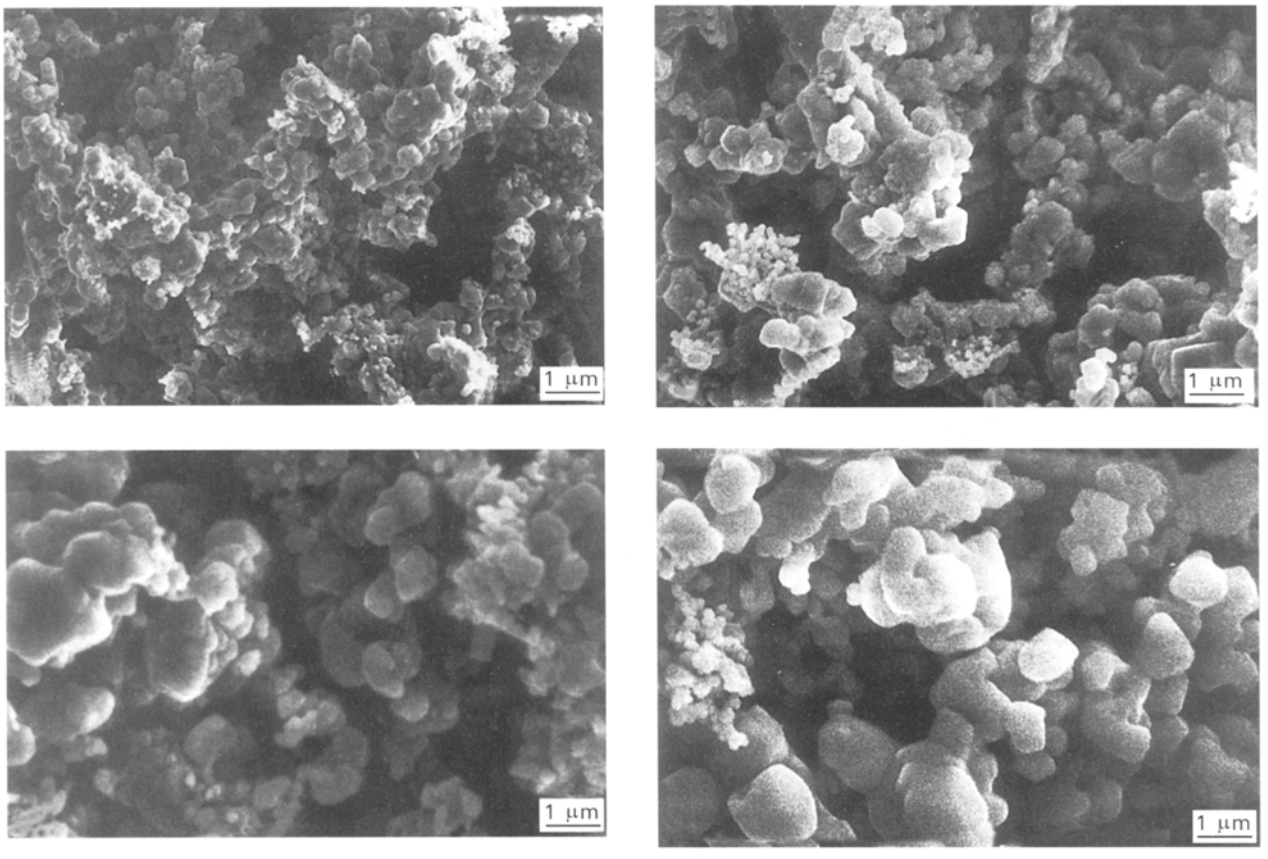

Figure 3 Scanning electron micrographs of α-Si_3N_4 from "as-is" pyrolysed rice hulls.

Figure 4 Transmission electron micrograph of α-Si_3N_4 from "as-is" pyrolysed rice hulls.

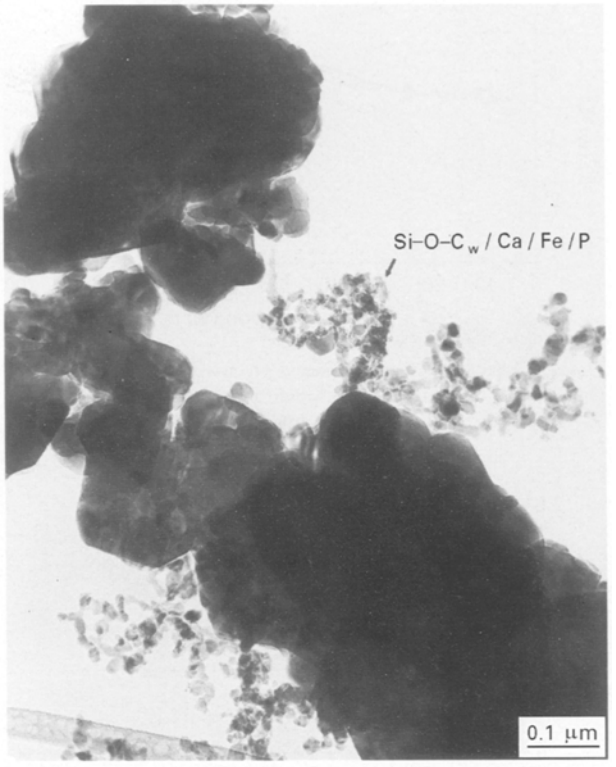

Figure 6 Transmission electron micrograph of α-Si_3N_4 crystallites from "as-is" pyrolysed rice hulls and amorphous Si–O–C "fluff" containing impurities Ca, Fe, and P.

magnifications and the TEM image shown in Fig. 4, indicate a bimodal α-Si_3N_4 particle-size distribution (PSD). The TEM (Fig. 4) indicates the crystallites to be rather solid and non-porous. The presence of ultra-fine α-Si_3N_4 crystallites was confirmed by electron diffraction (ED) (Fig. 5). A particle-size distribution analysis of the α-Si_3N_4 crystallites indicated the larger portion of the bimodal distribution of crystallites to be in a range of 0.08–0.47 μm with a mean size of 0.22 ± 0.08 μm (mean circle diameter, Russ [15]). The finer crystallites were in a range of 0.01–0.06 μm with a mean size of 0.03 ± 0.01 μm (unit size 34 nm; sizing based upon a mean circle diameter, Russ [15]).

Metallic impurities (Ca, Fe, P) were concentrated in an amorphous Si–O–C "fluff" (Fig. 6) which coated the Si_3N_4 crystallites in some areas. The "fluff" consisted of a chain-like structure of crystallites in a size range of 0.01–0.05 μm with a mean size of 0.02 ± 0.01 μm (unit size 26 nm). Metallic impurities were not detected within the Si_3N_4 crystallites.

3.1.1 Effect of per cent excess carbon and reaction temperature on burned out percentage of carbon and oxygen

The effect of excess carbon and temperature on the weight per cent of oxygen present after burn-out is minimal as can be seen from the results presented in Fig. 7. None of the precursors was capable of producing a final product with less than 3 wt% monatomic oxygen. The 5.8% excess carbon-containing precursor produced a product with 3.5 wt% oxygen at maximum run time and temperature. The 75% excess carbon produced a product with 4.2 wt% oxygen. These results indicate that the per cent excess carbon has a minimal effect on the amount of oxygen in the

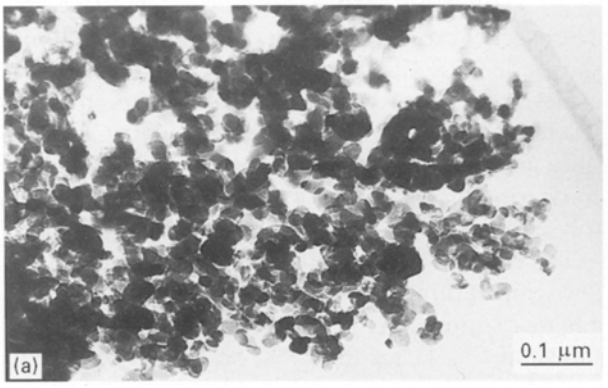

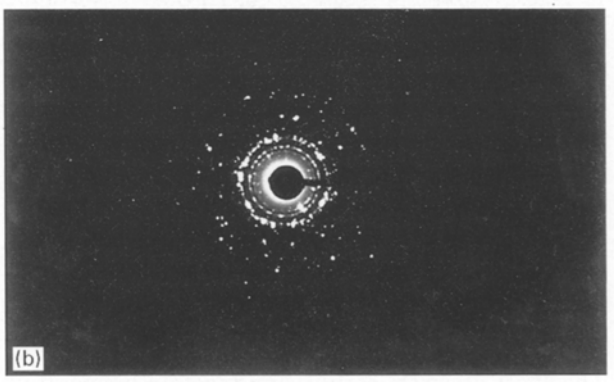

Figure 5 (a) Micrograph and (b) Electron diffraction pattern of ultra-fine α-Si_3N_4 powder from "as-is" pyrolysed rice hulls.

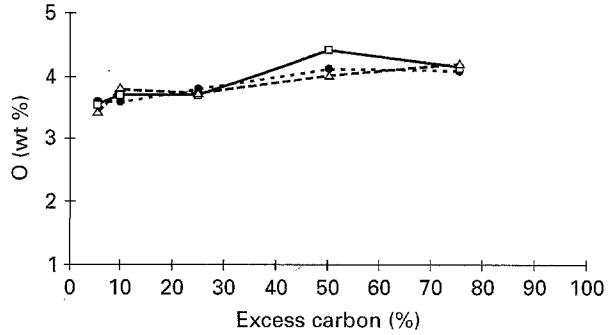

Figure 7 Effect of percentage excess precursor carbon content and temperature on final product weight per cent of oxygen (t = 5 h; T = (●) 1460, (□) 1480 and (△) 1500 °C; "seed"/SiO_2 = 0.2).

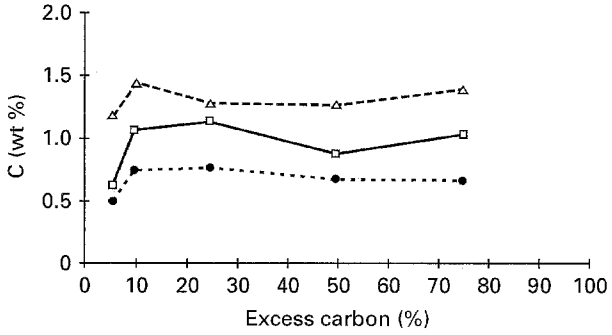

Figure 8 Effect of percentage excess precursor carbon content and temperature on final product weight per cent of carbon (t = 5 h; T = (●) 1460, (□) 1480 and (△) 1500 °C; "seed"/SiO_2 = 0.2).

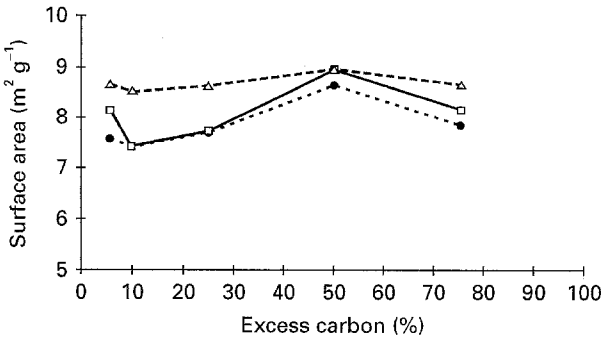

Figure 9 Effect of percentage excess precursor carbon content and temperature on final product surface area (t = 5 h; T = (●) 1460, (□) 1480 and (△) 1500 °C; "seed"/SiO_2 = 0.2).

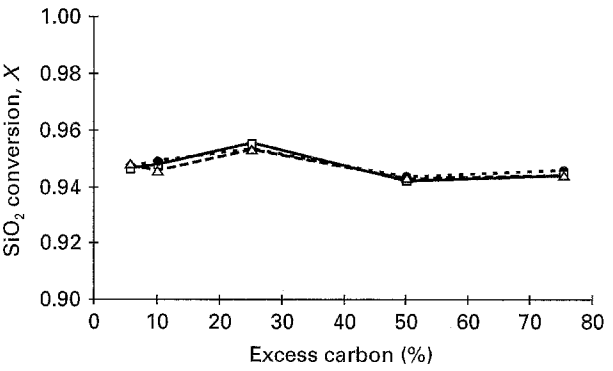

Figure 10 Effect of percentage excess precursor carbon content and temperature on silica conversion (t = 5 h; T = (●) 1460, (□) 1480 and (△) 1500 °C; "seed"/SiO_2 = 0.2).

final product. The results shown in Fig. 7 also indicate that reaction temperature (varied between 1460 and 1480 °C) had a minimal effect on the amount of oxygen in the final product.

The effect of excess carbon and temperature on the burned out weight per cent carbon is shown in Fig. 8. These results indicate that reaction of a low per cent excess-carbon (< 10%) precursor yields a final product powder having less residual carbon relative to that product produced from reaction of a precursor which contains the added higher excess carbon (> 10% excess). One reason for this finding may be the lack of intimacy of the added carbon black with the SiO_2 relative to the intimate C/SiO_2 mixture comprising the calcined rice hulls "as-is". There is little difference in the final carbon content for reaction of precursors containing carbon in the range of 10%–75% excess. The results shown in Fig. 8 also illustrate that the final product contains a higher weight per cent carbon if the precursor is reacted at a higher reaction temperature. It is believed that both high reaction temperatures and the presence of metal impurities in the pyrolysed rice hulls promote the formation of Si–O–C and SiC. Because all free carbon is presumably removed in the burn-out step, all remaining carbon is assumed to be in the form of Si–O–C and SiC.

3.1.2. Effect of excess carbon and reaction temperature on surface area

The effect of excess carbon and reaction temperature on surface area is shown in Fig. 9. There appears to be little effect on the final product surface area when the percentage of excess carbon in the precursor is increased. However, when the temperature was increased, an increase in the surface area was observed. This increase in surface area may be related to the fact that there is an increase in burned out weight per cent carbon with an increase in temperature. At higher temperatures, the formation of nanophase SiC was promoted, and because the particle size of nanophase Si–O–C and SiC is smaller than Si_3N_4, it would produce a higher surface area product.

3.2. Effect of percentage of excess carbon on reaction rate

3.2.1. Effect of precursor composition on reaction rate

The effect of excess carbon on the extent of reaction is shown in Fig. 10. A conversion above 94% was achieved for all precursors (all excess carbon levels) reacted for 5 h at temperatures above 1460 °C. A 95% silica conversion appears to be the upper limit of conversion for this series of experiments (reacting pyrolysed rice hulls with added seed).

The effect of reaction time on SiO_2 conversion for low temperature is shown in Figs 11 and 12. Clearly, a higher temperature increases the rate of reaction as shown in Fig. 11 for the 5.8% excess carbon precursor. The results shown in Fig. 12 indicate that there may be a slight increase in the rate of reaction (SiO_2

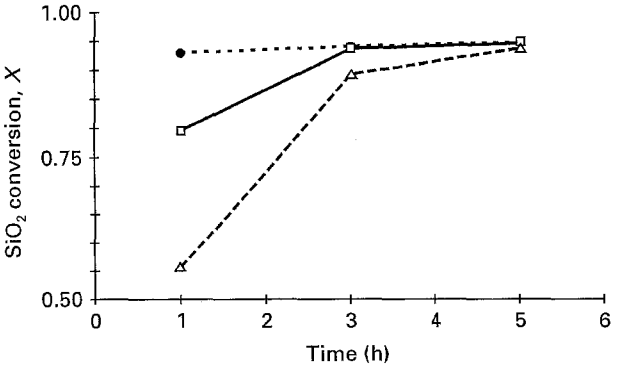

Figure 11 Effect of reaction time and temperature on silica conversion (5.8% excess C; T = (△) 1340, (□) 1380 and (●) 1420 °C; "seed"/SiO_2 = 0.2).

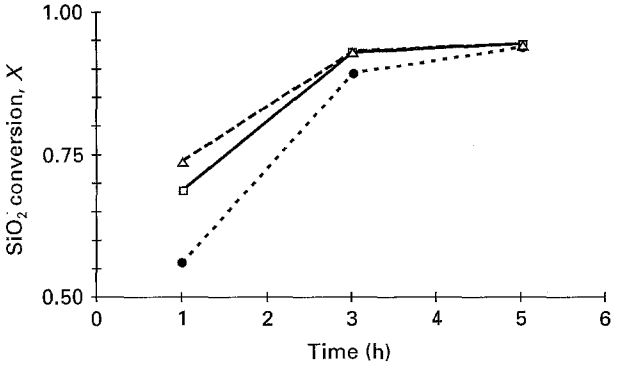

Figure 12 Effect of reaction time and excess percentage precursor carbon content on silica conversion (T = 1340 °C; excess C = (●) 5.8%, (□) 10% and (△) 25%; "seed"/SiO_2 = 0.2).

conversion) as the percentage of excess carbon is increased. However, the effect of reaction time and temperature are much more influential on conversion than the per cent excess carbon.

The results in Fig. 11 show that complete conversion can be obtained for the 5.8% excess carbon precursor (no added carbon) in approximately 3 h at 1380 °C.

3.2.2. Effect of reaction time and percentage of excess carbon on final product weight per cent oxygen and carbon at low temperatures

The results shown in Fig. 13 for the low-temperature reaction (1340 °C) indicate that the percentage of excess precursor carbon has little effect on the rate of reaction. However, there is a substantial effect of time at temperature. After 1 h reaction, there is approximately four times as much oxygen in the final product than after 3 and 5 h.

As shown in Fig. 14, the percentage of excess precursor carbon does not have a large impact on burned out weight per cent carbon. This observation is consistent with runs at higher temperatures. An interesting observation in Fig. 14 is that the amount of final carbon after burn-out generally decreases with an increase in reaction time. This result indicates that some intermediate carbon species (Si–O–C) may form

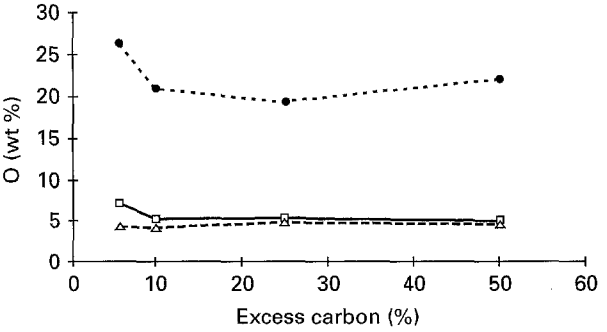

Figure 13 Effect of percentage excess precursor carbon content and reaction time on final product wt% oxygen (T = 1340 °C; t = (●) 1, (□) 3, and (△) 5 h; "seed"/SiO_2 = 0.2).

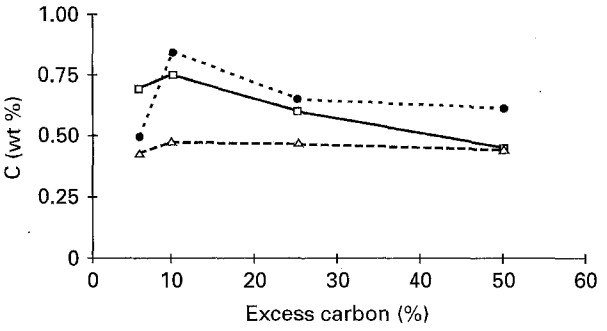

Figure 14 Effect of percentage excess precursor carbon content and reaction time on final product wt% carbon (T = 1340 °C; t = (●) 1, (□) 3, and (△) 5 h; "seed"/SiO_2 = 0.2).

quickly and then convert to Si_3N_4 upon additional reaction.

3.3. Reaction kinetics modelling

3.3.1. Nucleation–growth kinetics

The nucleation and growth effects are commonly combined into a single mechanism called nucleation kinetics. This mechanism has been used quite successfully in the study of phase changes (i.e. crystallization) or the decomposition of solid materials. An extensive explanation of this mechanism is given by Avrami [17–19]. Tompkins [20] indicated that the Erofeyev [21] approximation of Avrami's expression is adequate for describing most kinetic data of the nucleation type.

The form of the Erofeyev [21] equation is

$$(kt)^m = -\ln(1 - X) \tag{7}$$

where t is the time (s), m is a constant, X is the conversion, and k is the Arrhenius constant defined by the following equation

$$k = k_0 \exp(-E/RT) \tag{8}$$

where k_0 is the pre-exponential factor (s^{-1}), R the gas law constant (8.314 J mol^{-1} K^{-1}), T the temperature (K), and E the activation energy (J mol^{-1}).

The nucleation kinetics mechanism is based on the activation of reaction sites, followed by growth of the "product" nuclei through chemical reaction. The Avrami constant, m, accounts for the reaction mechanism, number of nuclei present, composition of parent

and product phases, and geometry of the nuclei. It indicates the order of the time dependence of the nucleation and the number of growth directions [22]. When nucleus activation is the rate-limiting step, $m \rightarrow 4$. When isotropic three-dimensional nucleus growth is the rate limiting step, then $m \rightarrow 3$. For one-dimensional rod-like growth control, $m \rightarrow 1$, while for two-dimensional planar growth control, $m \rightarrow 2$. For one-dimensional homogeneous parabolic growth as the rate-limiting step, $m \rightarrow 1/2$.

Avrami's equation can be transformed to make it suitable for multiple linear regression as follows

$$(kt)^m = -\ln(1 - X) \quad (9)$$

$$m\ln(k) + m\ln(t) = \ln[\ln(1/1 - X)] \quad (10)$$

$$\ln[\ln(1/1 - x)] = m\ln(k_0) - (Em)/(RT) + m\ln(t) \quad (11)$$

This is of the form

$$y = a_0 + a_1x_1 + a_2x_2 \quad (12)$$

$$a_0 = m\ln(k_0) \quad (13)$$

$$a_1 = -(Em)/R \quad (14)$$

$$a_2 = m \quad (15)$$

$$x_1 = 1/T \quad (16)$$

$$x_2 = \ln(t) \quad (17)$$

$$y = \ln\{\ln[1/(1 - X)]\} \quad (18)$$

3.3.2. Regression analysis

Only low conversion data from reaction of the 5.8% "as-is" precursor were used for the kinetic study. The results are $E = 420\,\text{kJ mol}^{-1}$, $k_0 = 1.09 \times 10^{10}\,\text{s}^{-1}$, and $m = 0.58$. The fit of predicted versus observed values for y, determined from Equation 18, is shown in Fig. 15. The activation energy of $E = 420\,\text{kJ mol}^{-1}$ for pyrolysed rice hulls is slightly lower than the activation energy reported for reaction of high-purity reactants [23]. The value $m = 0.58$ for the Avrami constant indicates that homogeneous parabolic growth dominates the process.

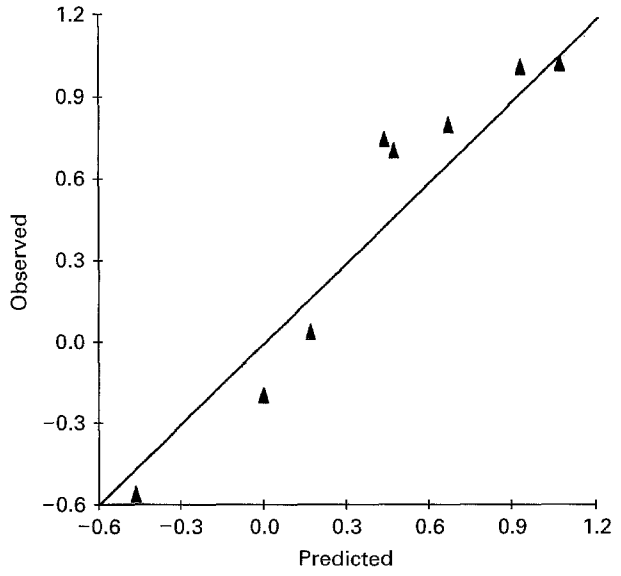

Figure 15 Predicted versus observed values for $y = \ln\{\ln[1/(1 - X)]\}$, Equation 18.

4. Conclusions

Pyrolysed rice hulls (pyrolysed in nitrogen) are an intimate C/SiO_2 source (providing excess carbon above the stoichiometric requirement) for the carbothermal nitridation synthesis of $> 95\%$ α-Si_3N_4. Carbothermal nitridation reaction (flowing nitrogen) of a precursor containing pyrolysed rice hulls and additive Si_3N_4 "seed" ("seed"/$SiO_2 = 0.2$) can be completed in approximately 3 h at 1380 °C. An activation energy of $420\,\text{kJ mol}^{-1}$ is lower than previous values reported for reaction of high-purity reactants [23]. The addition of carbon black to the pyrolysed rice hull C/SiO_2 mixture (to increase the amount of excess carbon in the precursor) is not necessary to complete the reaction or improve the product powder properties.

The product Si_3N_4 powder (after excess carbon removal by air oxidation) is less pure than that synthesized from higher purity starting materials, but may be suitable for low-temperature applications. It is $> 95\%$ α phase, has a surface area of $7.7\,\text{m}^2\,\text{g}^{-1}$, and contains 3.6 wt% monatomic oxygen, 0.5 wt% total carbon, 1900 p.p.m. Al, 2000 p.p.m. Fe, and 7900 p.p.m. Ca. The metallic impurities are concentrated in an amorphous Si–O–C "fluff" which coats the Si_3N_4 crystallites in some areas. The bulk of the powder is comprised of submicrometre solid α-Si_3N_4 crystallites having a bi-modal crystallite size distribution (0.22 ± 0.08 μm, 0.03 ± 0.01 μm). No whiskers or high aspect ratio elongated crystallites were detected in the product powder.

The carbothermal nitridation reaction of "seeded" ("seed"/$SiO_2 = 0.2$) pyrolysed rice hulls can be modelled using a nucleation–growth rate expression. The reaction can be described by

$$(kt)^{0.58} = -\ln(1 - X) \quad (19)$$

$$k = 1.09 \times 10^{10}\exp(-50\,502/T) \quad (20)$$

where T is the temperature (K), $(1573 < T < 1653)$, t the residence time (s), $(3600 < t < 18000)$, X the fractional SiO_2 conversion $(0 < X < 1)$, k = rate (s^{-1}).

Acknowledgement

This research was partially sponsored by the US Department of Energy, Assistant Secretary for Energy Efficiency and Renewable Energy, Office of Transportation Technologies, as part of the Ceramic Technology Project of the Propulsion System Materials Program, under contract DE-AC05-84OR21400 with Martin Marietta Energy Systems, Inc.

References

1. T. QUADIR, R. W. RICE, J. C. CHAKRAVERTY, J. A. BREINDEL, and C. C. WU, *Ceram. Eng. Sci. Proc.* **12** (1991) 1952.

2. B. K. PADHI and C. PATNAIK, *Ceram. Int.* **21** (1995) 213.
3. K. SATYANARAYANA, *Res. Ind.* **35**(12) (1990) 223.
4. D. F. HOUSTON, "Rice Chemistry and Technology" (American Association of Cereal Chemistry, St Paul, MN, 1972) p. 301.
5. S. B. HANNA, N. A. L. MANSOUR, A. S. TAHA and H. M. A. ABD-ALLAH, *Br. Ceram. Trans. J.* **84** (1985) 18.
6. S.-W. KANG and S.-S. CHUN, *J. Kor. Ceram. Soc.* **16**(2) (1979) 99.
7. N. KUSKONMAZ, C. TOY, O. ADDEMIR and A. TEKIN, in "Third Euro-Ceramics", Vol. 1, edited by P. Duran and J. F. Fernandez (Faenza Editrice Iberica, S. L., Spain, 1993) pp. 125–30.
8. J. G. LEE and I. B. CUTLER, *Am. Ceram. Soc. Bull.* **54**(2) (1975) 195.
9. Y. LI, L. LIU and S. DOU, *J. Inorg. Mater.* (*Wuji Cailiao Xuebao – Chinese*) **6**(1) (1991) 45.
10. N. A. L. MANSOUR and S. B. HANNA, *Br. Ceram. Soc. Trans. J.* **68**(6) (1979) 132.
11. M. PATEL and P. PRASANNA, *Interceram.* **40** (1991) 301.
12. I. A. RAHMAN and F. L. RILEY, *J. Eur. Ceram. Soc.* **5** (1989) 11.
13. R. F. RODRIGUEZ and R. F. J. NARCISO, *Anal. Quim.* **87** (1991) 788.
14. N. K. SHARMA and W. S. WILLIAMS, *J. Am. Ceram. Soc.* **67** (1984) 715.
15. J. C. RUSS, "Computer-Assisted Microscopy: The Measurement and Analysis of Images" (Plenum Press, New York, 1990).
16. M. TSUKADA, J. NAITO, T. MASUDA and M. HORIO, *Funtai Kogaku Kaishi* **26**(3) (1989) 157.
17. M. AVRAMI, *J. Chem. Phys.* **7** (1939) 1103.
18. *Idem, ibid.* **8** (1940) 212.
19. *Idem, ibid.* **9** (1941) 177.
20. F. C. TOMPKINS, in "Treatise on Solid State Chemistry", Vol. 4, "Reactivity of Solids", edited by N. B. Hannay (Plenum Press, New York, 1976) p. 206.
21. B. V. EROFEYEV, *C.R. Acad. Sci. URSS* **52** (1946) 511.
22. Z. STRNAD, "Glass-Ceramic Materials: Liquid Phase Separation, Nuleation and Crystallization in Glasses" (Elsevier, New York, 1986).
23. A. W. WEIMER, G. A. EISMAN, D. W. SUSNITZKY, J. W. McCOY and D. R. BEAMAN, *J. Am. Ceram. Soc.* (1996) in press.

Received 3 January
and accepted 18 March 1996